



Biological activity and preclinical efficacy of azetidiny pyridazines as potent systemically-distributed stearoyl-CoA desaturase inhibitors

Elise Isabel^{*}, David A. Powell, W. Cameron Black, Chi-Chung Chan, Sheldon Crane, Robert Gordon, Jocelyne Guay, Sebastien Guiral, Zheng Huang, Joël Robichaud, Kathryn Skorey, Paul Tawa, Lijing Xu, Lei Zhang, Renata Oballa

Merck Frosst Centre for Therapeutic Research, PO Box 1005, Pointe-Claire-Dorval, Québec, Canada H9R 4P8

ARTICLE INFO

Article history:

Received 14 September 2010

Revised 20 October 2010

Accepted 21 October 2010

Available online 26 October 2010

Keywords:

Stearoyl-CoA desaturase inhibitors

SCD

Pyridazine

Azetidine

Systemically-distributed

ABSTRACT

Potent and orally bioavailable SCD inhibitors built on an azetidiny pyridazine scaffold were identified. In a one-month gDIO mouse model of obesity, we demonstrated that there was no therapeutic index even at low doses; efficacy in preventing weight gain tracked closely with skin and eye adverse events. This was attributed to the local SCD inhibition in these tissues as a consequence of the broad tissue distribution observed in mice for this class of compounds. The search for new structural scaffolds which may display a different tissue distribution was initiated. In preparation for an HTS campaign, a radiolabeled azetidiny pyridazine displaying low non-specific binding in the scintillation proximity assay was prepared.

© 2010 Elsevier Ltd. All rights reserved.

The incidence of obesity and diabetes occurrence worldwide continues to increase at an alarming pace. The World Health Organization (WHO) has estimated that 1.6 billion adults are currently overweight with at least 400 million of these being classified as obese.¹ There is a strong risk factor for developing type 2 diabetes in obese individuals.² It has been hypothesized that de-regulation of stearoyl-CoA desaturase-1 enzyme (SCD, a delta-9 desaturase) may play an important role in the development of these metabolic disorders.³ SCD catalyzes the formation of a *cis*-double bond at the C-9 position of C-16 palmitoyl-CoA and C-18 stearoyl-CoA into palmitoleoyl-CoA and oleoyl-CoA, respectively.⁴ Four SCD isoforms have been characterized in mouse. Although they display a similar desaturation activity towards stearoyl-CoA and palmitoyl-CoA, they have a different tissue distribution.^{5,6} So far, two isoforms, SCD1 and SCD5, have been characterized in humans. Human SCD1 is the ortholog of the mouse SCD1, whereas SCD5 is not an ortholog of any of the four mouse enzyme and is highly expressed in brain and pancreas.⁷ Besides delta-9 desaturases, there are two other desaturases in humans: delta-5 and delta-6. Since these two desaturases are involved in the synthesis of highly unsaturated fatty acids which are esterified into phospholipids and contribute to maintain membrane fluidity, selectivity against delta-5 and delta-6 is essential to avoid undesirable toxicities.⁸ Recently, we and others disclosed several new classes of potent SCD inhibitors which

are capable of inhibiting SCD activity *in vivo* (Fig. 1).^{9–12} We demonstrated that efficacy in preventing weight gain in either a growing or established diet induced obesity model (gDIO or eDIO) tracked closely with partial eye closure and alopecia. We now report a complementary series, the azetidiny pyridazines. The purpose of this work was to identify a series that would allow for a therapeutic window by a titration of the dose of a systemically-distributed SCD inhibitor to the minimal amount required for efficacy in a gDIO model. Additionally, as a result of the unique physical properties of these inhibitors, specifically their low affinity for polyvinyltoluene (PVT) and yttrium silicate, a member of this series served as a key component in a recently-developed SPA binding assay.

Azetidiny pyridazines were synthesized following the general sequence described in Scheme 1. The commercially available 3-methyl-6-chloropyridazine was oxidized to the corresponding carboxylic acid **2**. The carboxylic acid was then converted into an acid chloride which was immediately reacted with acetic hydrazine in the presence of an organic base to obtain **3** in satisfactory yield over 2 steps. Compound **3** was reacted with Burgess's reagent (methyl *N*-(triethylammoniumsulfonyl)carbamate) at high temperature in the microwave to perform a dehydration/cyclization and provide the oxadiazole **4**. The commercially available Boc-protected 3-azetidinol **5** was reacted with phenols **6** under modified Mitsunobu conditions to yield ethers **7**.¹³ The Boc protecting group was removed in the presence of anhydrous HCl, and in most cases, the azetidine hydrochloride salt was isolated directly by filtration.

^{*} Corresponding author. Tel.: +1 514 428 3655; fax: +1 514 428 2624.

E-mail addresses: elise_isabel@merck.com, isabel.e@videotron.ca (E. Isabel).

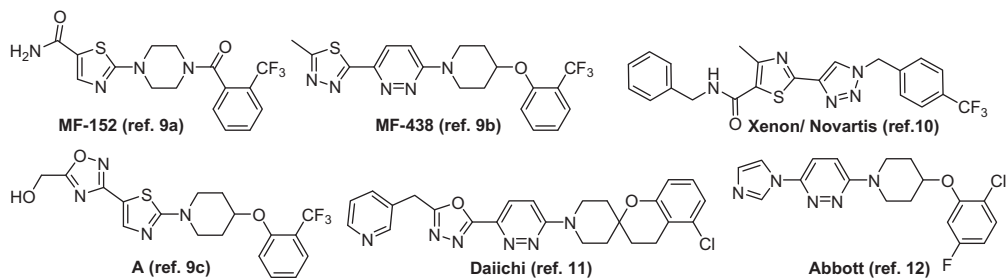
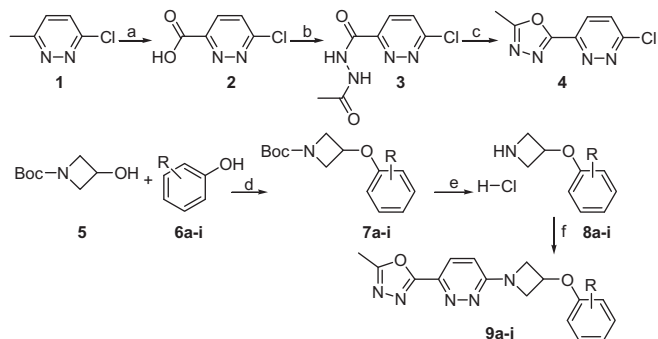


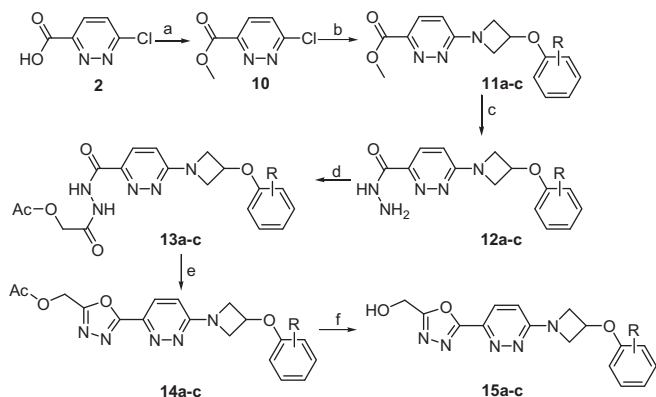
Figure 1. Recently published SCD inhibitors.



Scheme 1. Reagents and conditions: (a) potassium dichromate (1.2 equiv), H_2SO_4 , 50 °C, 4 h, 40% (b) (i) oxalyl chloride (1.1 equiv), DMF (cat.), toluene (ii) acetic hydrazine (1.2 equiv), Hunig's base (2.0 equiv), dichloromethane, 0 °C, 1.5 h, 54% (c) Burgess's reagent (1.5 equiv), THF, 150 °C (microwave), 30 min, 97% (d) phenol (1.2 equiv), 1,1'-(azodicarbonyl)dipiperidine (1.2 equiv), tri-*n*-butylphosphine (1.2 equiv), THF, 16 h, 75 °C, 47% (e) 4 M HCl in dioxane (5.0 equiv), dichloromethane, 83% (f) **4** (1.0 equiv), K_2CO_3 (3.0 equiv), dioxane, 110 °C, 2 days, 40%. Yields given for R = *ortho*- CF_3 .

The synthesis was completed by a thermal displacement step in refluxing dioxane to afford the desired compounds (**9a–i**) in acceptable yields.

SCD inhibitors **15a–c** were synthesized according to the sequence of reactions shown in Scheme 2. The carboxylic acid **2** was converted into an acid chloride with oxalyl chloride in the presence of a catalytic amount of DMF. After 1 h, the volatile components were removed under reduced pressure. The acid chloride was dissolved in toluene, cooled to 0 °C and MeOH was added to provide the methyl ester **10**. Thermal displacement with the



Scheme 2. Reagents and conditions: (a) (i) oxalyl chloride (1.1 equiv), DMF (cat.), toluene, 1 h (ii) MeOH (28 equiv), toluene, 2 h, 0 °C, 70%; (b) **8** (1.0 equiv), K_2CO_3 (3.0 equiv), dioxane, 110 °C, 2 days, 50%; (c) hydrazine (20 equiv), EtOH, 16 h; (d) acetoxyacetyl chloride (1.2 equiv), dichloromethane/water 2:3, 2 h, used unpurified; (e) Burgess's reagent (1.2 equiv), THF, 150 °C (microwave), 30 min, 51%; (f) hydrazine (10 equiv), MeOH, 16 h, 75%. Yields given for R = *ortho*- CF_3 .

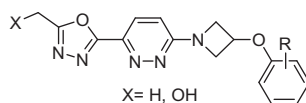
appropriate azetidines **8** was successfully achieved to provide the pyridazines **11a–c**. Acylhydrazides **12a–c** were obtained by reacting the methyl esters with a large excess of hydrazine in EtOH as a co-solvent. The terminal nitrogen of the hydrazines **12a–c** was then acylated with acetoxyacetyl chloride to give the doubly acylated hydrazides **13a–c**. Compounds were then subjected to a dehydration/cyclization sequence with the Burgess's reagent to yield the oxadiazoles **14a–c**. Finally, the deprotection of the acetate group on the primary alcohol with hydrazine provided compounds **15a–c**.

Azetidine inhibitors **9a–i** and **15a–c** were tested in a rat liver microsomal enzyme assay.¹⁴ The cellular potencies against SCD and selectivities against the delta-5 and delta-6 desaturases (data not shown, all analogs tested were inactive, >2 μM) were measured in a HepG2 whole cell assay.¹⁵ The results of these experiments are shown in Table 1. When compared to **MF-438**, **9a** was approximately 12-fold less potent in the enzyme assay but had a comparable potency in the cellular assay. The SAR in this series followed a similar trend to those previously reported, with *ortho*-substitution on the aryl ether ring providing the most potent compounds.⁹ Compound **9g** with a *meta*-substituted trifluoromethyl group was far less active in the enzyme assay and addition of an *ortho*-substituent to the *meta*-substituted CF_3 (**9h**) was not sufficient to restore potency. Evaluation of the pharmacokinetics properties of **9d** and **9e** in mice revealed that these azetidiny analogs have a similar long half-life as the piperidine derivatives (7 h versus 6.4 h for **MF-438**).¹⁶ LC-MS analysis of the whole blood samples identified a M+16 metabolite circulating with the parent compound. Based on previous observations with **MF-438** and **A**, it was suspected that this metabolite was being generated by the enzymatic oxidation of the methyl moiety of the oxadiazole to the corresponding alcohol.⁹ Considering that this alcohol functionality did not negatively impact the potency of previous analogs, these primary alcohols (**15a–c**) were prepared so that they could be evaluated. Compound **15a** exhibited a comparable potency to **MF-438** against the rat enzyme with a similar bioavailability and half-life. When comparing **15a** to **9a**, it seems clear that adding the primary alcohol moiety provided a marked improvement in intrinsic potency. Compounds **15b** and **15c** had similar potencies in the enzyme assay, but there was almost a 10-fold difference in the whole cell assay, **15b** being the most potent (5.6 nM).

Having identified the azetidiny pyridazines as potent and bioavailable SCD inhibitors, we next sought to choose a suitable inhibitor for evaluation in an in vivo anti-obesity mouse model study and assess if a therapeutic window could be established. Lead compounds **15a** and **15c** were further profiled in a mouse liver pharmacodynamic model (mLPD) in order to measure in vivo inhibition of liver SCD activity.¹⁴ We had previously found that compounds which exhibit a high inhibition in our mLPD demonstrate efficacy in anti-obesity models. Inhibitors **15a** and **15c** were administered orally in 1% methocel. One hour later, ^{14}C -stearic acid (SA) was intravenously administered in 60% PEG-200. Two hours following the administration of the tracer, livers were harvested.

Table 1

Potency and mouse pharmacokinetics data of azetidinyl piperazine SCD inhibitors



| Compd | X | R | Rat SCD enz. IC ₅₀ (nM) ^a | HepG2 cell IC ₅₀ (nM) ^a | Mouse PK (%F; t _{1/2} in h) ^b |
|---------------|----|-------------------------|---|---|---|
| MF-438 | H | 2-CF ₃ | 2.3 | 21 | 73; 6.4 |
| 9a | H | 2-CF ₃ | 27 | 9.0 | 75; 2.8 |
| 9b | H | 2-Br | 21 | 23 | n.d. |
| 9c | H | 2-I | 7.2 | 22 | n.d. |
| 9d | H | 2-Br, 5-F | 28 | 19 | 97; 6.9 |
| 9e | H | 2-Br, 4-F | 67 | 40 | 91; 7.7 |
| 9f | H | 2-Cl, 5-CF ₃ | 163 | n.d. | n.d. |
| 9g | H | 3-CF ₃ | 1992 | n.d. | n.d. |
| 9h | H | 2-Cl, 3-CF ₃ | 3385 | n.d. | n.d. |
| 9i | H | 2-Cl, 4-F, 6-Cl | 8167 | n.d. | n.d. |
| 15a | OH | 2-CF ₃ | 2.3 | 13 | 57; 5.0 |
| 15b | OH | 2-Br, 5-F | 3.4 | 5.6 | 61; 4.4 |
| 15c | OH | 2-Br | 4.9 | 50 | 100; 2.2 |

^a IC₅₀'s are an average of at least two independent titrations.^b 10 mg/kg PO (1% methocel, n = 2) and 2 mg/kg IV (60% PEG-200, n = 2).

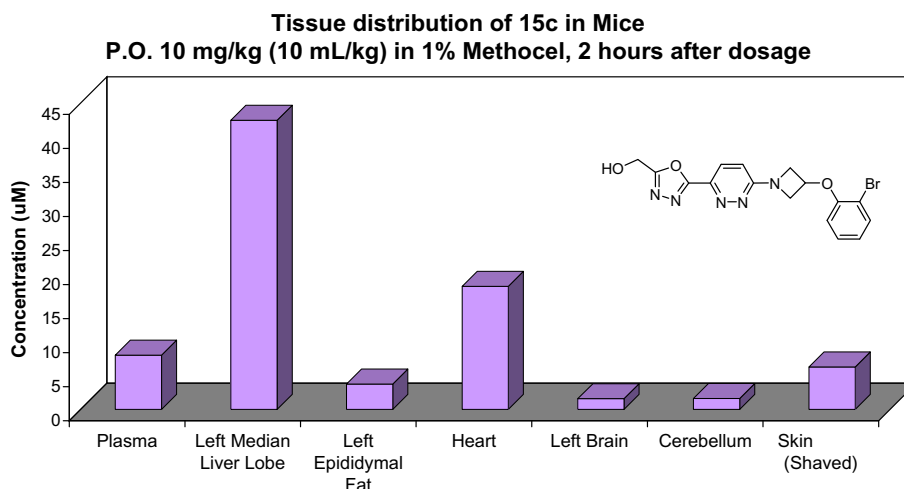
After a basic hydrolysis of liver lipids, samples were analyzed with a radiometric detector. Since SCD effects the conversion of stearic to oleic acid (OA), low levels of OA characterize a potent SCD inhibitor. As reported in Table 2, **15c** was demonstrated to be a more potent inhibitor of liver SCD activity in vivo as compared to **15a**. Compound **15c** achieved a >90% suppression of oleic acid production at a dose of 1 mg/kg, 3-fold lower than that required to

observed comparable effect on oleic acid production with **15a**. A tissue distribution study (Fig. 2) with **15c** was conducted and confirmed that **15c** retains a systemically-distributed tissue profile with a 4.5-fold higher drug concentration being observed in the liver compared to plasma, similar to **MF-438** and **A**. Compound **15c**, as a result of its potent in vivo activity, was evaluated in a one-month growing diet induced obesity model (gDIO) in mice. Our goal was to down titrate **15c** to see if at low exposure it was possible to avoid adverse effects previously observed with **A** (0.2 mg/kg) and **MF-438** (5 mg/kg). The doses chosen for this study with **15c** were 0.1 and 0.3 mg/kg qd. The highest dose was selected in order to provide full inhibition of liver activity (as demonstrated in the mLPD assay) while the low dose was chosen at 1/3 of the high dose where only partial inhibition of liver SCD activity is observed. Results are shown in Figure 3. When **15c** was administered at 0.1 mg/kg/day, there was a moderate, but statistically significant improvement in body weight over the control group ($P < 0.01$) after 28 days. No eye adverse effects (AE's) were observed with 0.1 mg/kg/day of **15c** for the duration of the study.¹⁷ However after 3 weeks of treatment, skin AE's were observed. With a dose of 0.3 mg/kg/day of **15c**, AE's were comparable to what was observed

Table 2mLPD assay: in vivo SCD inhibition of **15a** and **15c**

| Compd | Dose (mg/kg) | % Inhibition ^a | Plasma and liver levels (μM) |
|------------|--------------|---------------------------|------------------------------|
| 15a | 3.0 | 97% ($P = 0.044$) | 1.9; 15.8 |
| 15a | 1.0 | NS | 0.01; 7.9 |
| 15a | 0.3 | NS | 0; 1.2 |
| 15c | 1.0 | 92% ($P < 0.001$) | 1.4; 11.9 |
| 15c | 0.3 | 74% ($P < 0.001$) | 0.1; 7.2 |
| 15c | 0.1 | NS | 0; 2.7 |

NS = Non-significant.

^a SCD activity index (ratio of ¹⁴C-oleic acid/¹⁴C-stearic acid) in hydrolyzed liver lipids; n = 5 per group.**Figure 2.** Tissue distribution 2 h post-dose at 10 mg/kg PO in C57BL6 mice fed on normal chow diet.

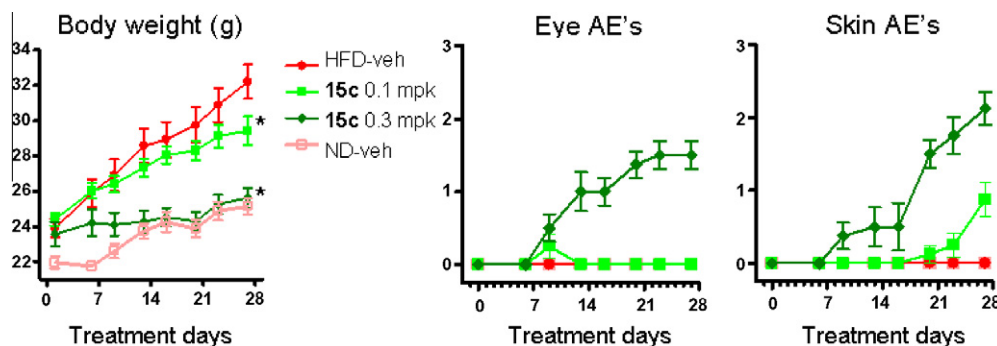


Figure 3. Body weight gain, eye AE's and skin AE's of C57BL/6 mice fed on high fat diet and dosed qd with **15c** compared to two control arms: fed on high fat and normal chow over 4 weeks; $n = 8$ per group; HFD-veh = high fat diet, vehicle treated control group; ND-veh = normal diet, vehicle treated control group.

previously with **MF-438** and **A**. Based on this data, it was concluded that obtaining a beneficial effect for reduced weight gain without experiencing AE's with a systemically-distributed compound was likely not possible (Fig. 3).

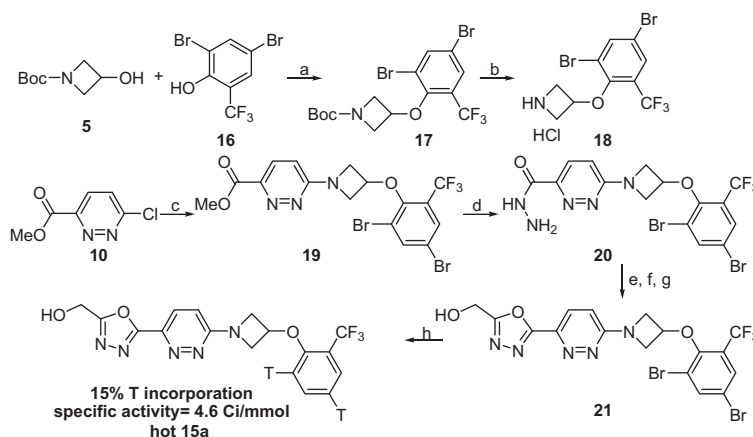
Since the azetidinyl pyridazine series and other systemically-distributed series were not providing an adequate therapeutic window, there was a need to identify new scaffolds. We felt that new scaffolds which offer a different tissue distribution profile may provide a suitable therapeutic window to enable clinical development. A high throughput screening campaign using a scintillation proximity binding assay (SPA) was put in place to evaluate our in-house small molecule collection for activity against SCD. A suitable compound to support the development of a SPA binding assay had to be identified. Such a compound should have good potency against SCD (i.e., <50 nM) and give low non-specific binding with the scintillation proximity beads. Unfortunately, previously identified series demonstrated significant binding to plate and gave high

non-specific binding with various types of scintillation proximity beads. The azetidinyl piperazines display increased water solubility and possess a measured $\log D_{7.4}$ of less than 1.0, in contrast to all other SCD inhibitors available in-house. A preliminary test in the presence of TBS buffer¹⁸ in a plastic eppendorf tube demonstrated that the azetidinyl piperazines **15a** and **15c** were recovered in high yields. For inhibitors tested from other series available in-house (results not shown) there was less than 30% recovery (Table 3).¹⁹ Once it was discovered that **15a** and **15c** were adhering less to plastic, **15c** was used to test two types of scintillation beads: PVT and yttrium. From this experiment, PVT-WGA and yttrium silicate-antimouse beads were chosen for further investigation. Even though **15c** had a slightly greater recovery in the first round of experiment (**15a**: 69% versus **15c**: 79% recovery), it became clear that it would be a greater synthetic challenge to obtain a radiolabeled version of **15c** while maintaining the *ortho*-bromine. We decided to revisit **15a** under the best conditions identified with

Table 3
Identification of a suitable compound for the development of a SPA binding assay

| | % Recovery in TBS | | | % Recovery for beads and media with 15c ^a | | | | | | | % Recovery with optimized conditions | |
|------------|-------------------|-----------|------------|---|---------|---------|---------|---------|---------|---------|--------------------------------------|--------------------|
| | 15c | 9c | 15a | Cond. 1 | Cond. 2 | Cond. 3 | Cond. 4 | Cond. 5 | Cond. 6 | Cond. 7 | 15a PVT | 15a Yttrium |
| Concn (nM) | 79 | 42 | 69 | 70 | 66 | 50 | 96 | 98 | 89 | 112 | 29 | 84 |

^a Cond. 1: 3 mg of PVT-PEI-WGA type A beads into 200 μ L of TBS buffer. Add 2 μ L of **15c** (10 μ M DMSO). Shake for 5 min, centrifuge at 12,000 rpm for 1 min, remove supernatant (~ 150 μ L) and analyze by LC-MS using a standard curve. Cond. 2: 3 mg of PVT-PEI-WGA type B beads and proceed as in cond. 1. Cond. 3: 3 mg of PVT-WGA beads and proceed as in cond. 1. Cond. 4: 9.5 mg of yttrium silicate-WGA beads and proceed as in cond. 1. Cond. 5: 9.5 mg of yttrium silicate-poly-L-lysine beads and proceed as in cond. 1. Cond. 6: 100 μ L of yttrium silicate-antimouse beads + 5 μ L of TBS buffer. Add 1 μ L of **15c** (10 μ M DMSO). Shake 5 min, centrifuge at 12,000 rpm for 1 min, remove supernatant (~ 90 μ L). Cond. 7: 100 μ L of yttrium silicate-antimouse beads + 5 μ L of 0.15 mg/mL mouse-anti-Flag antibody and proceed as in cond. 6.



Scheme 3. Reagents and conditions: (a) **5** (2.3 equiv) phenol (1.0 equiv), 1,1'-(azodicarbonyl)dipiperidine (3.0 equiv), tri-*n*-butylphosphine (3.0 equiv), THF, 16 h, 75 °C, 85%; (b) 4 M HCl in dioxane (5.0 equiv), dichloromethane, 4 h, 71%; (c) **18** (1.0 equiv), **10** (1.5 equiv), K_2CO_3 (3.0 equiv), dioxane, 110 °C, 24 h, 74%; (d) hydrazine (20 equiv), EtOH, 24 h, 92%; (e) acetoxyacetyl chloride (1.2 equiv), dichloromethane/water 2:3, 0.5 h, 0 °C, used crude; (f) Burgess's reagent (1.3 equiv), dioxane, 120 °C, 2 h, 26% over 2 steps; (g) hydrazine (10 equiv), MeOH, 16 h, 75%; (h) $Pd(OH)_2$ on carbon (2.6 equiv), Et_3N (13 equiv), T_2 (60 mm Hg), EtOH/THF 5:1, 16 h, 35%.

15c. Although low recovery was obtained with **15a** in the presence of PVT beads, an acceptable 84% recovery was observed with yttrium beads. Following this, a radiolabeled synthesis of **15a** was designed (Scheme 3). A Mitsunobu-type reaction between **5** and **16**²⁰ was performed in refluxing THF for 2 days to give the ether **17** in an 85% yield. The Boc group was cleaved in a few hours at room temperature in presence of HCl to provide the hydrochloride salt **18** as a white solid. The azetidine **18** and the chloropyridazine **10** were reacted with potassium carbonate in refluxing dioxane for 24 h. The intermediate **19** was obtained in a 74% yield and was further reacted with excess hydrazine to provide the hydrazide **20** in a high yield of 92%. The terminal nitrogen of **20** was reacted with acetoxyacetyl chloride to give the doubly acylated intermediate which was used crude for the cyclization with Burgess's reagent. This provided the oxadiazole **21** in a 26% yield over two steps. The primary alcohol was deprotected in presence of a large excess of hydrazine. The last step of the synthesis was the incorporation of two tritium atoms on **21**. This was achieved with an excess of Pd(OH)₂ on carbon and T₂ in a 5:1 EtOH/THF solvent mixture. Compound **15a** was obtained in 35% yield after HPLC purification with 15% tritium incorporation. This compound was an effective ligand in an in-house SPA-based HTS campaign.²¹

In conclusion, we demonstrated that with a systemically-distributed azetidiny pyridazine SCD inhibitor it was not possible to maintain weight gain benefits in mice without also negatively affecting skin and eye functions. As a result, there is a need to identify new scaffolds displaying a differing tissue distribution profile and the preparation of a radiolabeled SCD inhibitor which serves as a probe for a SPA binding assay in an HTS campaign is disclosed. Full details about this work will be reported shortly.

References and notes

- World Health Organization, Fact sheet No. 311, September 2006 (data available at www.who.int).
- World Health Organization, Fact sheet No. 312, November 2009 (data available at www.who.int).
- Liu, G. *Expert Opin. Ther. Patents* **2009**, *19*, 1169.
- Ntambi, J. M. *Prog. Lipid Res.* **1995**, *34*, 139.
- Ntambi, J. M.; Miyazaki, M. *Curr. Opin. Lipidol.* **2003**, *14*, 255.
- Miyazaki, M.; Jacobson, M. J.; Man, W. C.; Cohen, P.; Asilmaz, E.; Friedman, J.; Ntambi, J. M. *J. Biol. Chem.* **2003**, *278*, 33904. and references cited therein.
- Wang, J.; Yu, L.; Schmidt, R. E.; Su, C.; Huang, X.; Gould, K.; Cao, G. *Biochem. Biophys. Res. Commun.* **2005**, *332*, 735.
- Nakamura, M. T.; Nara, T. Y. *Annu. Rev. Nutr.* **2004**, *24*, 345.
- (a) Li, C. S.; Belair, L.; Guay, J.; Murgasova, R.; Sturkenboom, W.; Ramtohl, Y. K.; Zhang, L.; Huang, Z. *Bioorg. Med. Chem. Lett.* **2009**, *19*, 5214; (b) Léger, S.; Black, W. C.; Deschênes, D.; Dolman, S.; Falgout, J.-P.; Gagnon, M.; Guiral, S.; Huang, Z.; Guay, J.; Leblanc, Y.; Li, C. S.; Masse, F.; Oballa, R. M.; Zhang, L. *Bioorg. Med. Chem. Lett.* **2010**, *20*, 499; (c) Ramtohl, Y. K.; Black, W. C.; Chan, C.-C.; Crane, S.; Guay, J.; Guiral, S.; Huang, Z.; Oballa, R. M.; Xu, L.; Zhang, L.; Li, C. S. *Bioorg. Med. Chem. Lett.* **2010**, *20*, 1593.
- Dales, N.; Zhang, Z.; Fonarev, J.; Fu, J.; Kamboj, R.; Kodumuru, V.; Pokrovskaya, N.; Sun, S. WO 2008/074835.
- Uto, Y.; Ueno, Y.; Kiyotsuka, Y.; Miyazawa, Y.; Kuruta, H.; Ogata, T.; Yamada, M.; Deguchi, T.; Konishi, M.; Takagi, T.; Wakimoto, S.; Ohsumi, J. *Eur. J. Med. Chem.* **2010**, *45*, 4788.
- Liu, G.; Lynch, J. K.; Freeman, J.; Liu, B.; Xin, Z.; Zhao, H.; Serby, M. D.; Kym, P. R.; Suhar, T. S.; Smith, H. T.; Cao, N.; Yang, R.; Janis, R. S.; Krauser, J. A.; Cepa, S. P.; Beno, D. W. A.; Sham, H. L.; Collins, C. A.; Surowy, T. K.; Camp, H. S. *J. Med. Chem.* **2007**, *50*, 3086.
- Tsunoda, T.; Yamamiya, Y.; Itô, S. *Tetrahedron Lett.* **1993**, *34*, 1639.
- Li, C. S.; Ramtohl, Y.; Huang, Z.; Zhang, L.; Lachance, N. WO 2006/130986.
- Zhang, L.; Ramtohl, Y.; Gagné, S.; Styhler, A.; Wang, H.; Guay, J.; Huang, Z. *J. Biomol. Screening* **2010**, *15*, 169.
- Bateman, K. P.; Castonguay, G.; Xu, L.; Rowland, S.; Nicoll-Griffith, D. A.; Kelly, N.; Chan, C.-C. *J. Chromatogr. B* **2001**, *754*, 245.
- A scoring system was implemented to evaluate the severity of the AE's: a score of 1 represents light AE's whereas severe AE's were given a score of 3.
- 50 mM of tris-(hydroxymethyl)aminomethane and 150 mM of NaCl. pH adjusted to 7.6 with HCl.
- Two sets of samples were analyzed. Sample set 1 was a 100 nM solution of the SCD inhibitor in 100 µL of a 1:1 EtOH/TBS buffer mixture. Sample set 2 was a 100 nM solution of the inhibitors in 100 µL of TBS buffer. Solutions were prepared in plastic eppendorfs. For each sample, 45 µL of solution was pipetted out using MAXIMUM RECOVERY (marketed by AXYGEN) 200 µL pipette tips to a glass vial with a built-in insert. Forty-five micro liters of acetonitrile containing and internal standard (IS) were added. Vials were capped, vortexed and used as is. Each sample was done in duplicate. For data analysis, the concentrations from the sample set 1 were set at 100 nM (no external quantitative standards) and runs from sample set 2 were then a direct comparison of peak area (standardized with an IS).
- Adams, A. D.; Green, A.I.; Szcwyczyk, J. W. WO 2007/064553.
- Skorey, K. in preparation.